

PROJECT TITLE: Non-contact system for thoracic activity monitoring

TEAM LEADER: Daniel TEICHMANN (Daniel.Teichmann@rwth-aachen.de)

TEAM MEMBERS: Jérôme FOUSSIER, Jing JIA

ADVISING PROFESSOR: Prof. Steffen LEONHARDT

UNIVERSITY: Chair for Medical Information Technology (MedIT)
RWTH Aachen University, Germany

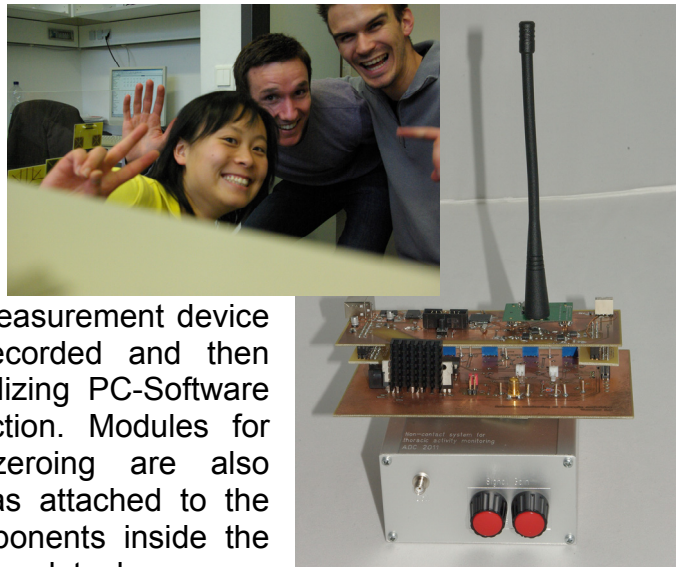
DATE: 20.07.2011

TI PARTS USED IN PROJECT:

- 1 C1101EMK433 <http://focus.ti.com/docs/toolsw/folders/print/cc1101emk433.html>
- 2 MSP430F5437A <http://focus.ti.com/docs/prod/folders/print/msp430f5437a.html>
- 1 CD74HCT4046A <http://focus.ti.com/docs/prod/folders/print/cd74hct4046a.html>
- 2 DCP021212D <http://focus.ti.com/docs/prod/folders/print/dcp021212d.html>
- 3 OPA890 <http://focus.ti.com/docs/prod/folders/print/opa890.html>
- 9 OPA132 <http://focus.ti.com/docs/prod/folders/print/opa132.html>

PROJECT ABSTRACT

A system for non-contacting monitoring thoracic activity is presented. It is based on magnetic induction measurement using an amplitude and phase modulation technique in order to render the possibility of working at a constant working frequency. The developed measurement device is integrated into a chair. The recorded and then processed signal is sent to a visualizing PC-Software either via wireless or USB connection. Modules for automatic calibration and filter zeroing are also implemented. Special importance was attached to the use of highly precise and fast components inside the radio frequency measurement parts and to low power consumption in general as the application is intended to be powered by battery. Analytic as well as simulative analyses have been carried out. Good functionality of the system was attested by measurements on a human volunteer.



Introduction

In personal healthcare long-term monitoring of respiratory and cardiac activity is highly important. Respiration and pulse can be monitored via the impedance fluctuation within the thorax. This can be achieved in a non-contacting way by magnetic eddy-current induction. In this work we have developed a system using this method. The measurement system has been applied to a chair, so that it is possible to monitor the respiratory activity of the person sitting on it. The recorded signal is filtered by analog and digital filter stages and transmitted wireless to a PC for visualization. The optimal working point is ensured by an automatic calibration routine realized by the use of a microcontroller.

Since the measurement system works with high frequencies (6-14 MHz) and the desired information has to be obtained from very small amplitude and phase changes, special characteristics of the electrical components are required.

Furthermore, for the purpose of using the device in mobile scenarios low power consumption is highly demanded.

In the following sections the theoretical background and a description of the developed system will be given. Simulative analysis (performed with TINA-TI), which was necessary during the design process in order to find the optimal devices and component values as well as to ensure analog circuitry functionality, are also presented. The used components and their advantages towards the design will be pointed out.

Finally, some results of the experimental evaluation are presented.

Motivation for Project

A few single coil systems for respiration and pulse monitoring based on magnetic eddy current induction are known from literature. They all have in common that they are based on a frequency modulated technique. Using this technique an alternating magnetic field is sent out by the use of an oscillatory circuitry which is detuned by thoracic activity. The resulting frequency variation is the obtained signal. This implies that the frequency of the magnetic field changes during the measurement, which could yield to poor linearity, because biological tissue shows frequency dependent conductivity and penetration depth.

Thus, a system providing the possibility of measuring body impedance changes by magnetic eddy current induction while keeping the sending frequency of the magnetic field constant would be advantageous. This was the main reason for the measurement system developed in this project.

In the system described here, an amplitude modulated signal is derived and the sending frequency can be kept constant, so that changes due to the frequency dependency of biological tissue are eliminated.

Furthermore, we wanted to be sure that the measured signal is not only dependent on thorax-motion, but also sensitive to changes in the inner thoracic conductivity distribution. This is why the sensor was attached to a rigid chair back-rest, in order to reduce motion of the thoracic wall towards the sensor.

Theoretical Background

Magnetic Induction

The physical principle of the coupling between a coil sending out an alternating magnetic field and a conductive object in its vicinity is shown in Figure 1 and is shortly described in the following. Driving an alternating current I_{coil} in a coil excites an alternating magnetic field B_{prim} . This excitation field induces an alternating voltage U_{ind} into the body which drives eddy currents I_{eddy} within the conductive tissue. These eddy currents again re-excite a secondary alternating magnetic field B_{sec} which correlates with thoracic conductivity and opposes the primary one. Hence, the superposition of both magnet fields can be measured within the coil.

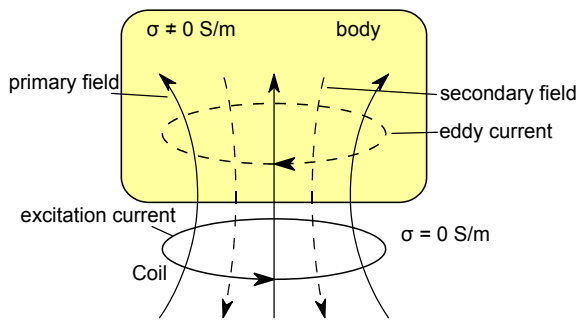


Figure 1 Physical principle

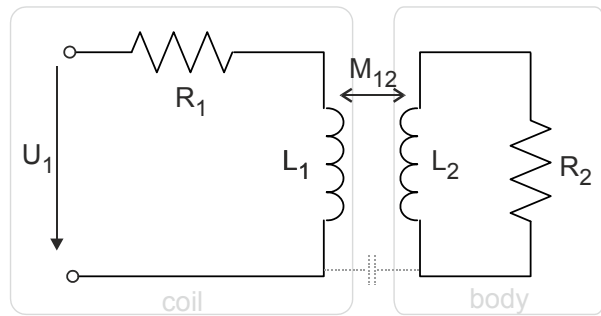


Figure 2 Equivalent transformer model

Physiological activity modifies the conductivity distribution within the thorax and therewith produces a variation of the re-excited magnetic field B_{sec} . This is due to variations of tissue impedance at certain regions and organ displacements.

The principle described above resembles an electronic transformer. The sensing coil forms the primary self-inductance L_1 and the eddy currents in its collective form the secondary one L_2 . This transformer circuitry is illustrated in Figure 2. The resistance R_1 is the series resistance of the sensing coil while R_2 gives a description of the eddy current losses within the conductive tissue. Both meshes are electromagnetically coupled via the mutual inductance $M_{12}=M_{21}$.

Complex Impedance and Resonant Frequency

In general, a complex impedance is described as $\underline{Z} = R + iX = Z_0 e^{-i\varphi}$, where R is defined as the resistance, X the reactance, Z_0 the impedance magnitude and φ the phase. If X now consists of a capacitive and non-ideal inductive component (see Figure 3), a resonant

frequency $f_r = \frac{1}{2\pi} \sqrt{\frac{1}{LC} - \left(\frac{R_L^2}{L}\right)}$ can be found.

At this frequency the impedance value has its maximum Z_r . Around the frequency f_x the slope of the impedance change ($\Delta Z/\Delta f$) is maximal and shows almost linear behavior.

This region is important for the measurement system as it has the highest sensitivity to impedance changes. A change in the inductance L , the capacitance C or the serial

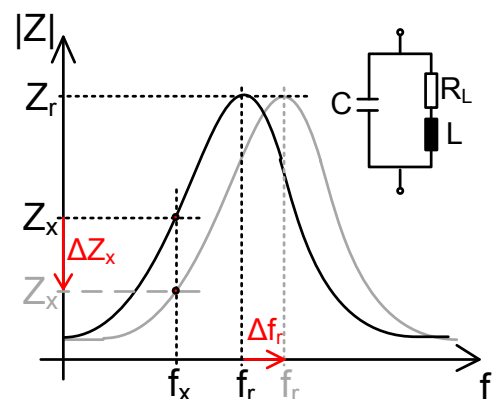


Figure 3 Parallel resonance

resistance R_L of the coil results in a resonant frequency change Δf_r , shifting the whole f - Z -curve to the left or to the right (see gray curve), and also in an impedance change of ΔZ_x . The frequency of the excitation voltage \underline{U}_0 of a voltage divider with the resistance R_0 (see Figure 4) is fixed to f_x and the system measures the impedance changes induced by physiological activity:

$$\underline{S} = \frac{U_L}{U_0} = \frac{Z}{Z + R_0} = \frac{R + iX}{R + iX + R_0} = \frac{R(R + R_0) + X^2 + iXR_0}{(R + R_0)^2 + X^2}$$

which leads to the real and imaginary parts of \underline{S} or alternatively to the amplitude and phase components of \underline{S} :

$$\Re\{\underline{S}\} = \frac{R(R + R_0) + X^2}{(R + R_0)^2 + X^2} \quad \Im\{\underline{S}\} = \frac{XR_0}{(R + R_0)^2 + X^2}$$

$$|\underline{S}| = \sqrt{\Re\{\underline{S}\}^2 + \Im\{\underline{S}\}^2} \quad \varphi_S = \arctan\left(\frac{\Im\{\underline{S}\}}{\Re\{\underline{S}\}}\right)$$

The above formulas show the dependency of X and R both in the amplitude and the phase of the signal \underline{S} . This points out, why it is beneficial to be able to measure both. The built up measurement system is able to measure those signals as described in the following section.

Implementation

Analog and Digital Circuitry

Heart of the circuitry is a TI microcontroller MSP430F5437A, running at 25 MHz. It is responsible for the communication with the PC, the measurement of the analog voltages, the calibration of the analog circuitry, controlling of the input voltage of a Voltage Controlled Oscillator (VCO) and the digital processing of the acquired data. The MSP430F5437A offers the maximal flexibility with its high-speed quartz crystal operation and its large amount of flash/SRAM space. It is possible to integrate some computationally intensive processing algorithms and a graphical visualization of the data on a small display, so that the system can be built up in an autarkic way. A system overview is given in the block diagram in Figure 4.

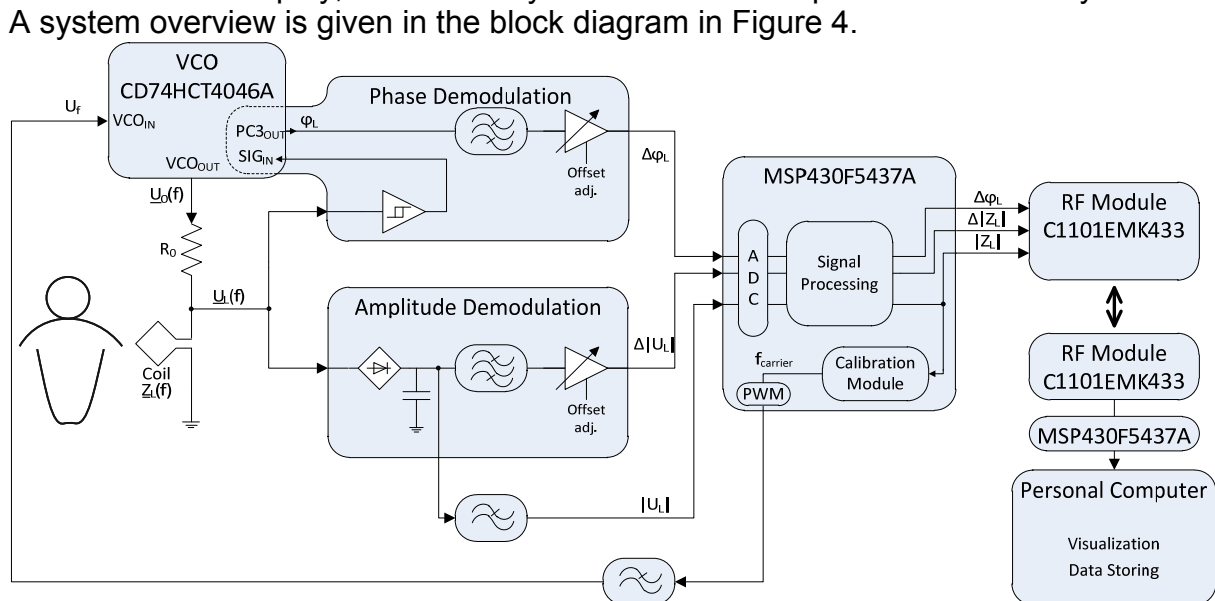


Figure 4 Block diagram of the developed measurement system

The microcontroller controls the input voltage of a Voltage Controlled Oscillator (VCO, TI part CD74HCT4046) with the use of a low-pass filtered PWM signal. The VCO is configured with $R_1=3\text{ k}\Omega$, $R_2=30\text{ k}\Omega$ and $C_1=100\text{ pF}$ as external components to cover a wide frequency range (center frequency $10\text{ MHz} \pm 4\text{ MHz}$). The output of the VCO is connected to a frequency dependant voltage divider, consisting of a resistor and the measurement coil (see Figure 4).

In Figure 5 the schematics of the analog board is presented. The realized combination of the analog and digital board is shown in the figure on the cover page.

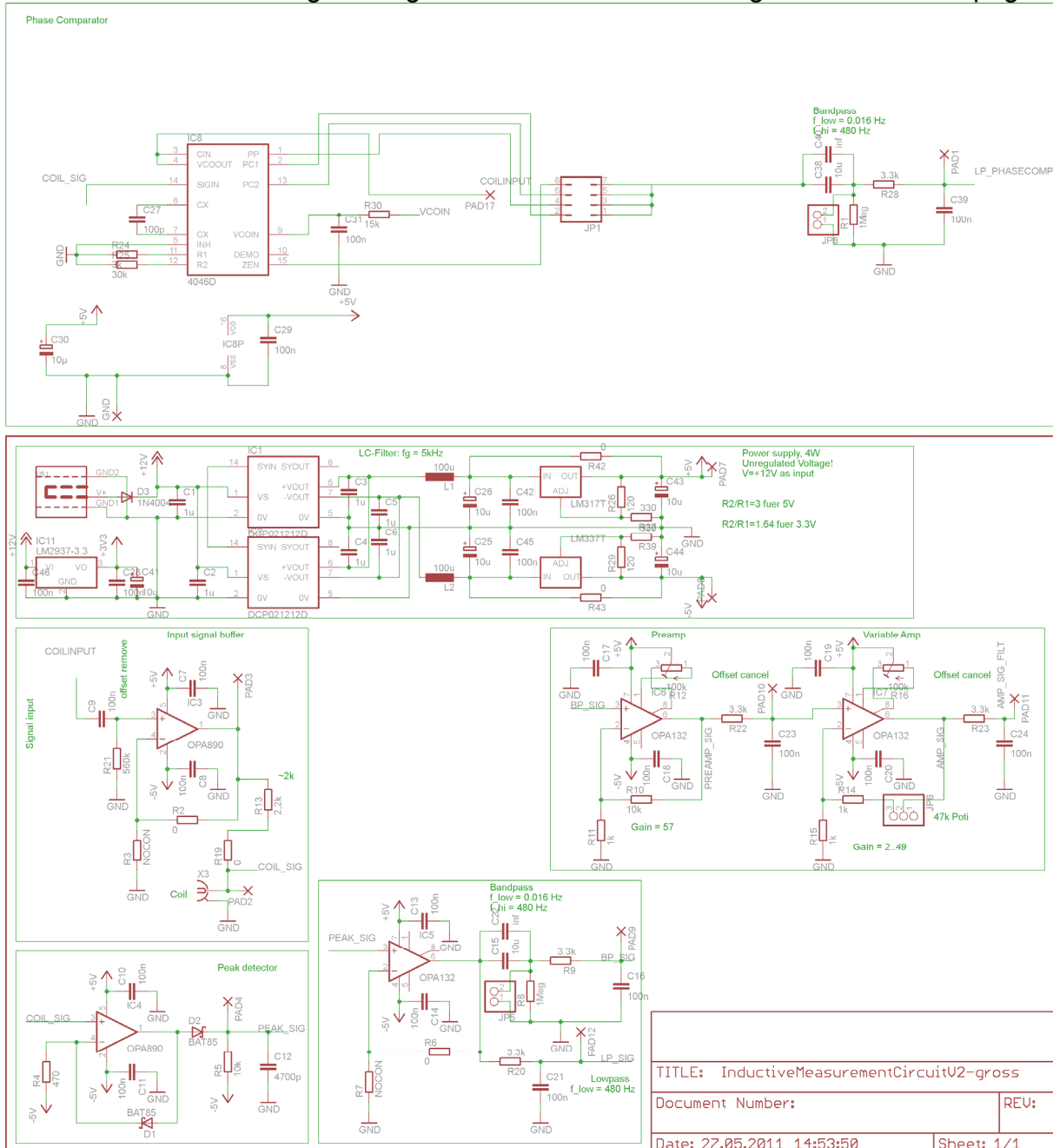


Figure 5 Schematics of the analog board
top: VCO circuitry; bottom: amplitude demodulation, active band pass & amplification

Amplitude and Phase Demodulation

The amplitude and phase information of the coil signal are determined by amplitude and phase demodulation, respectively.

For amplitude demodulation, the coil signal is passed to an active peak detector giving the peak amplitude at the output. The operational amplifier rapidly charges a capacitor smoothing the peaks to a continuous amplitude signal. This procedure is also called amplitude demodulation, as the desired signal is modulated on a high frequency signal. At this stage, the demodulator must be able to handle high frequency signals. Therefore, operational amplifiers with high slew rates are needed. The TI OPA890 have a 115 MHz wideband application range with a slew-rate of 500 V/μs, enough for the above stated purposes without neglecting the need of low power consumption. To optimize the necessary components of the amplitude demodulation, a simulation in TINA-TI has been performed. The schematic and the generated results can be found in Figure 6 and Figure 7, respectively. Note, that the amplitude demodulation settles within a few microseconds to the desired amplitude (red line), which is fast enough for our field of application. Also the ripple can easily be filtered out with a low-pass filter, as its carrier signal (green line) has a frequency of a few MHz. Since the OPA890 is not available in TINA-TI, we used the OPA690 which has similar characteristics except its lower speed. Hence, the assumption seems valid, that the circuitry simulated with the OPA690 should even work better using the OPA890.

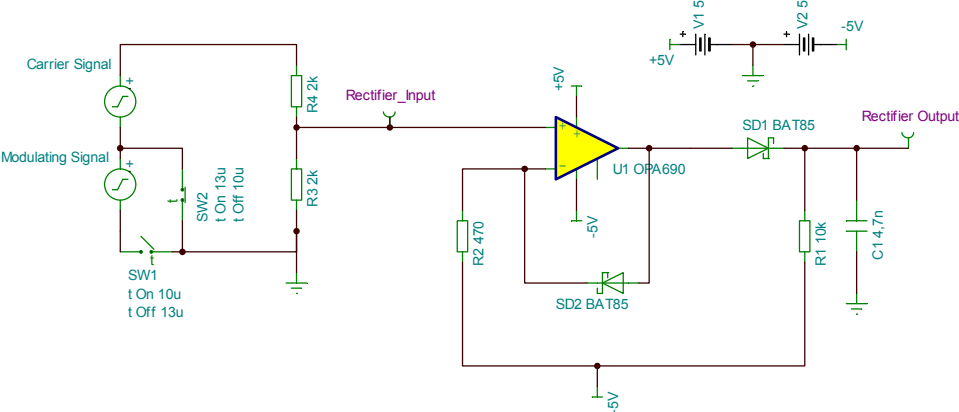


Figure 6 Test circuit for amplitude demodulation simulation

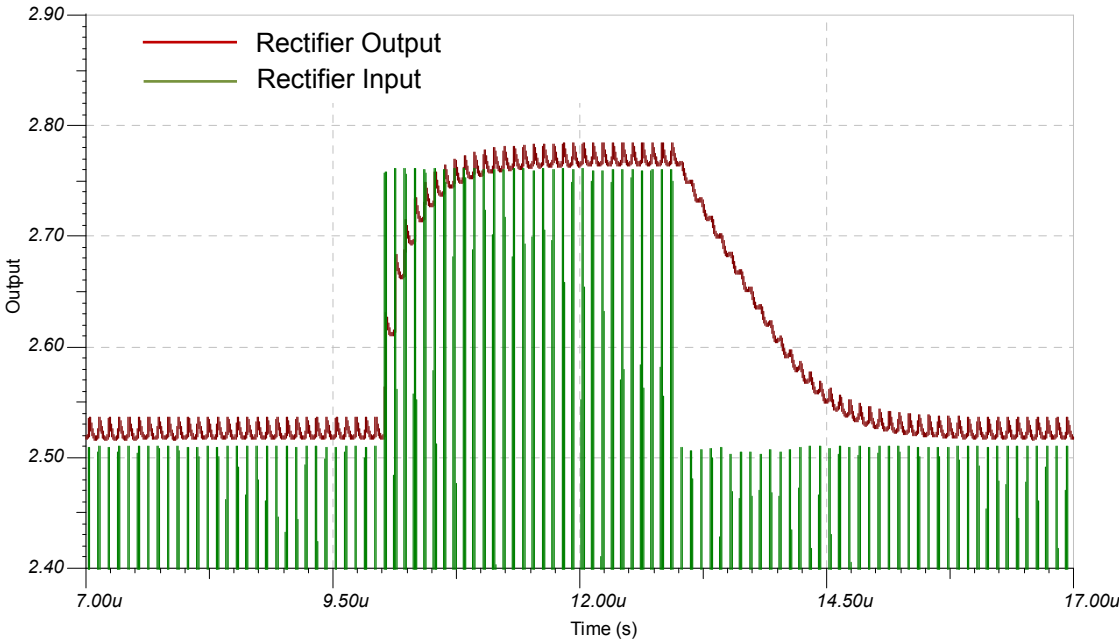


Figure 7 Result of amplitude demodulation simulation

An advantage of the CD74HCT4046 is that it provides – next to its VCO – three different phase comparators, since it can be used as a phase-locked loop circuit. For our purposes, we use the phase comparator for phase demodulation. The coil signal is processed into a square wave signal by Schmitt triggering and is passed to the signal input SIG_{IN} of the CD74HCT4046. In this way, it is possible to obtain the phase difference between the carrier signal produced by the VCO and the coil signal by using the PC3 output pin.

Empirical measurements showed maximal signal amplitude changes of about 5 mV_{pp} at the output of the amplitude demodulation, which is too small for the Analog-Digital-Converter in the MSP430 (12 bit at 1.25 V reference give a resolution of 0.3 mV/bit, thus only 4-5 bits remain for the desired signal). In addition, the DC voltage of over 2.5 V makes it impossible to directly connect the measured voltage to the ADC, as the reference voltage is set to 1.25 V for best resolution. Therefore, in the amplitude as well as in the phase demodulation path the need of analog circuitry for DC offset removal and signal amplification is essential. The first step is realized as a CR-RC band-pass filter with corner frequencies $f_L=0.016$ Hz and $f_H=480$ Hz. The lower corner f_L has to be set that low because the normal breathing rate is in the order of 0.1-0.2 Hz. This induces very long settling times ($\tau_L \approx 10$ s) which causes the system to be very slow. To overcome the long settling times, an automatic zeroing circuitry triggered by the microcontroller shunts the high-pass component for a short time, rapidly setting the filter output to 0 V, which is the reference voltage of the operational amplifiers. Once settled, the second step is to amplify very small signal changes and hence to extend the measurement range from a few mV_{pp} to maximum 8 V_{pp} (gain > 1600). The amplification has to be realized with two separate TI OPA132, because of the gain-bandwidth-product limitation of 8 MHz. The first amplifier has a fixed gain of 57 and the second a variable gain of 2-49, which the user can vary with a potentiometer. The OPA132 has been chosen as operational amplifier because it has very low noise, low distortion, low offset voltage and the ability to externally compensate the offset by an offset cancellation circuit, which is important when using these large amplification values (e.g. a 2 mV offset at the input would result in an output offset of more than 100 mV at gain 57).

The offset cancellation has to be adjusted by varying a potentiometer connected between the two “Offset Trim Pins”. As a first step towards the analog design this variable amplified band pass filter stage was also simulated using TINA-TI (see Figure 8 and Figure 9).

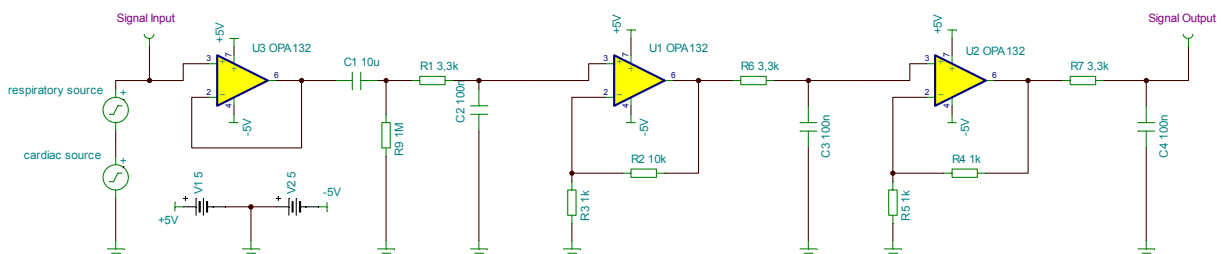


Figure 8 Test circuit for the variable amplified band pass stage simulation

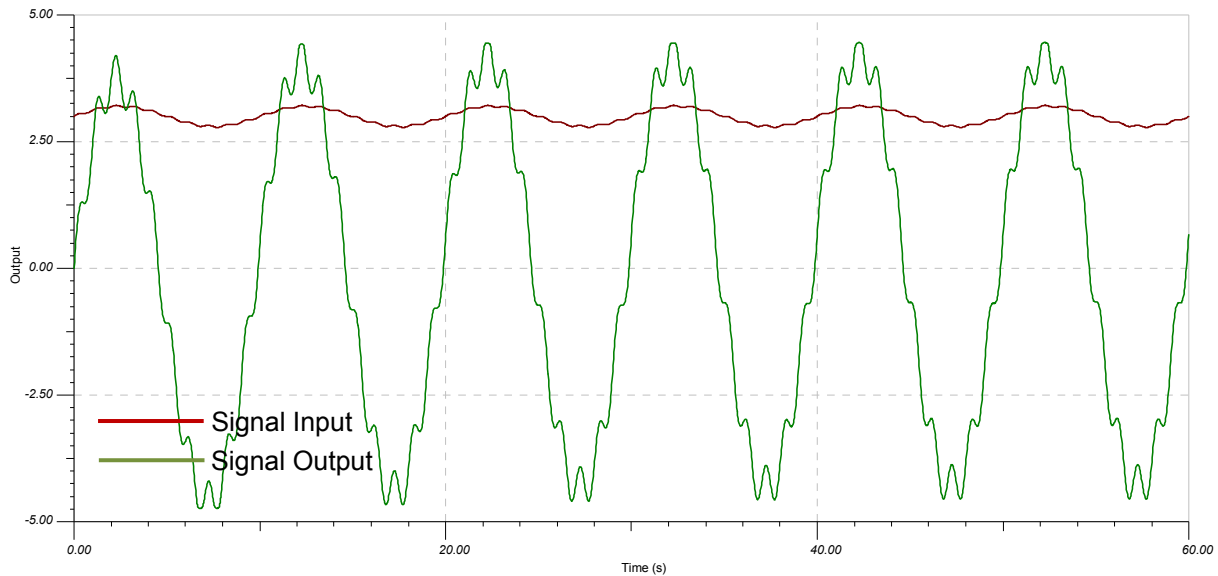


Figure 9 Result of the variable amplified band pass stage simulation

Power Supply

The whole circuitry is powered by two high efficient TI DC-DC converters (DCP021212D), connected together via the synchronization pin to obtain a maximal output power of 4 W. They can handle input voltages up to 15 V so that they are ready-to-use for a lead-acid battery as source for example. The unregulated dual outputs of ± 12 V are first filtered with an LC filter to reduce ripple. Then they are down-converted to stabilized ± 5 V with default voltage regulators, which are needed for the operational amplifiers employed in the amplification and voltage buffer stages of the analog signal processing. In a worst case scenario all the amplifiers drain up to 500 mA at ± 5 V supply, so the need of two DC-DC converters is evident.

Calibration

Due to non-idealities in the coil (serial resistance, parasitic capacitance ...), a parallel resonating circuit is formed with unknown resonant frequency. This frequency can range from 6 up to 14 MHz, depending on the shape and structure of the employed coil and the objects in its vicinity. The impedance of the non-ideal coil is maximal at the resonant frequency f_r . At startup, the calibration process in the MSP automatically sweeps the VCO control voltage from 0 to 5V, to determine the optimal excitation frequency f_x . With a 16 bit PWM signal, an average frequency resolution of $8 \text{ MHz} / 2^{16} \text{ bits} = 122 \text{ Hz/bit}$ is achievable. As described above (see Figure 3), the maximal sensitivity is reached at f_x , just before this resonant frequency. Nevertheless, the impedance changes remain very small.

Data Transmission

All signals recorded by the MSP430F5437A are wirelessly transmitted inside the 433 MHz band between the two RF modules of the C1101EMK433 kit which can communicate with the MSP430F5437A using the SPI interface. On the receiver side a second microcontroller module including the MSP430F5437A has been developed to connect it to a PC. The transmitted data is stored and visualized online via a graphical user interface. It is also possible to directly connect the measurement board to the PC via USB link.

Experimental Results

Calibration Procedure

In Figure 10 the envelope of the coil voltage signal during a calibration routine is presented. The frequency sweep is conducted correctly by linearly increasing the input voltage of the VCO in 6.5 seconds. During the linear frequency sweep, the signal amplitude follows the resonance curve described in Figure 3. After the frequency sweep, the frequency producing the maximum amplitude is chosen as the working frequency, which can be seen in the VCO input voltage step at second 6.5.

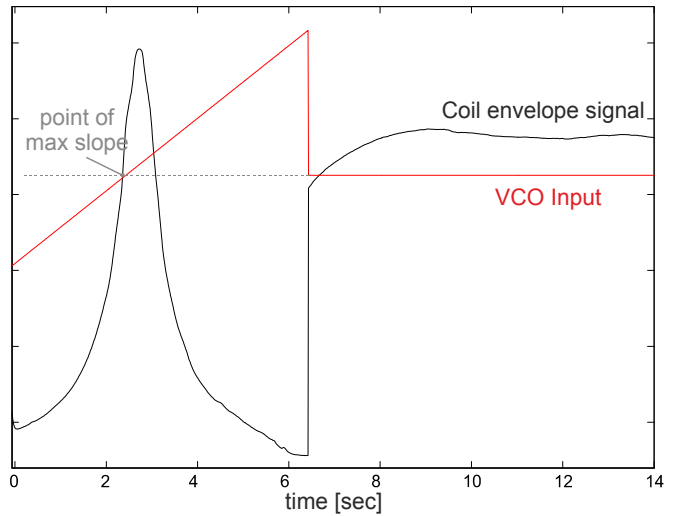


Figure 10 Calibration routine at startup

Measurement of a Healthy Volunteer

In order to attest the system’s functionality, we attached the sensor coil on the back rest of a chair and measured pulse and respiration of a person sitting on the chair. This setup can be seen in Figure 11.

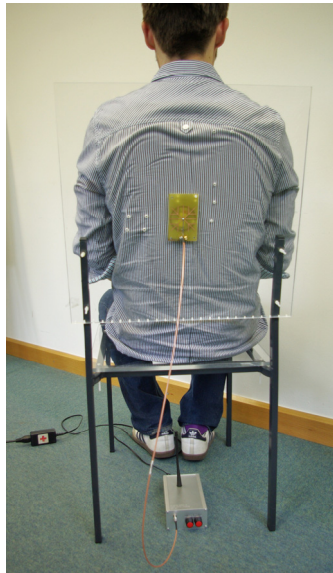


Figure 11 Measurement setup

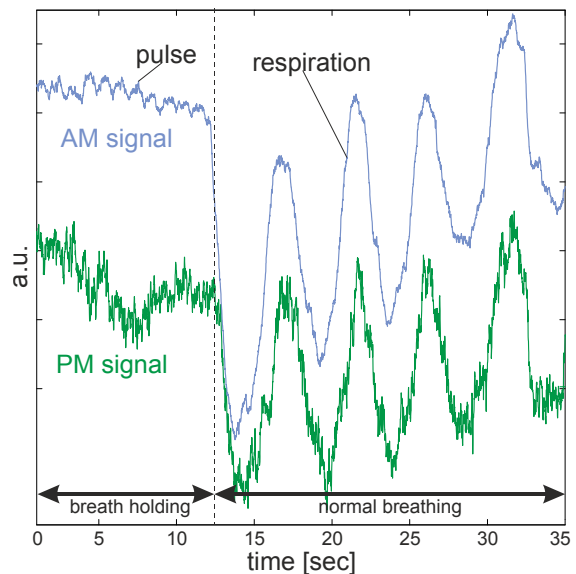


Figure 12 Measurement of human subject (AM = Amplitude Modulated; PM = Phase Modulated)

In Figure 12 an exemplary measurement during breath holding and normal respiration is presented. Both the amplitude modulated (AM) and phase modulated (PM) signals are plotted without any further post-processing on PC. Pulse is clearly visible during the breath holding phase, but also during respiration the superimposing cardiac related signal content is still noticeable. The PM signal is less sensitive than the AM signal. A rough estimate yields to SNR values of $SNR_{AM}=23.5$ dB and $SNR_{PM}=13.9$ dB in respect to respiration.

Summary & Conclusions

In this project a system for non-contact measurement of thoracic activity, i.e. respiration and pulse has been developed.

An essential part of the system is the automatic calibration routine which correctly determines the resonance frequency of the sensor coil.

Information about the coil impedance is obtained by amplitude and phase demodulation. The amplitude demodulator works well and in accordance to simulations conducted with TINA-TI. Phase demodulation was possible by using the phase difference input and phase error detection of the CD74HCT4046.

In order to measure the very small signal changes aroused by thoracic activity, extensive filtering and amplification strategies on analog level were undertaken and good results have been achieved.

All data were recorded by a MSP430F5437A and were sent via 433 MHz to a PC with help of the C1101EMK433.

Future Plans

Several steps towards a better differentiation between respiration and cardiac related signal contents are thinkable. Different sending frequencies could be systematically investigated concerning their sensitivity to the heart signal (mainly due to different penetration depths). In analogy, different coil positions could be investigated concerning the same information. Furthermore, a combination of several coils would be possible to combine their signals in order to assess more information about heart and lung activity.

A second challenge is the occurrence of motion artifacts due to the parasitic stray capacitance between coil and thorax surface. Therefore, it should be more focused on the capacitive shielding of the sensor.

It is furthermore imaginable to implement a breathing and heart rate detection algorithm in the microcontroller which sends its results to a remote device. The remote device does not necessarily have to be a PC. As the CC1101 wireless transmission chip is employed, a connection to the TI ez430-Chronos watch is also possible, enhancing the portability of the whole measurement system and making it independent from external processing units.